ISSN 1808-8546 (ONLINE) 1808-3765 (CD-ROM)

DISTRIBUIÇÃO DE ÁGUA DE MICROASPERSOR PARA DIFERENTES CONDIÇÕES OPERACIONAIS

GIULIANI DO PRADO[1]; TIAGO BUENO BRAGA COELHO[1]; ADRIANO CATOSSI TINOS[1]; DENISE MAHL[1] E EDMILSON CESAR BORTOLETTO[1]

[1] Departamento de Engenharia Agrícola - DEA, Universidade Estadual de Maringá - UEM, Rodovia PR 482, km 45, CEP: 87.820-000, Cidade Gaúcha-PR, Brasil. E-mail: gprado@uem.br, buenotiagobc@gmail.com, actinos@uem.br, demahl@gmail.com, ecbortoletto@uem.br.

1 RESUMO

O trabalho objetivou avaliar o microaspersor Naan Hadar®, modelo 7110, operando na ausência de ventos. Ensaios laboratoriais de distribuição de água foram realizados para 144 condições operacionais de: pressões de serviço (10, 15 e 20 mca), diâmetros de bocais (0,9; 1,0; 1,1 e; 1,2 mm), tipos de insertos (nebulizador - INeb e pequeno alcance - IPalc), alturas de instalação (0,5; 1,0, 1,5 m) e posições verticais (cima e baixo). A altura de instalação proporcionou maiores variações no raio de alcance para o IPalc posicionado para cima (23,4%) do que para baixo (1,3%), para o INeb, essas variações foram de 0,7 a 2,9%. Seis formas geométricas do perfil radial adimensional foram suficientes para caracterizar o microaspersor operando com o INeb e IPalc. Nas simulações da distribuição de água para diferentes arranjos de espaçamentos retangulares e triangulares, verificou-se que: o INeb, independentemente da altura e posição do microaspersor, com espaçamentos próximos a 50% do diâmetro molhado (DM), resultam em elevados valores de coeficiente de uniformidade (CU), e; para o IPalc, a posição do microaspersor para baixo deve ser preferida, pois resulta em altos valores de CU para espaçamentos até 60% do DM.

Palavras-chave: altura de instalação, pressão de serviço, diâmetro de bocal.

PRADO, G; COELHO, T. B. B.; TINOS, A. C.; MAHL, D; BORTOLETTO, E. C. MICRO-SPRINKLER WATER DISTRIBUTION FOR DIFFERENT WORKING CONDITIONS

2 ABSTRACT

The study aimed to evaluate the Naan Hadar® micro-sprinkler, model 7110, working in no-wind conditions. Laboratory tests of water distribution were performed for 144 working combinations, given by: working pressures (10, 15, and 20 mwc), nozzle diameters (0.9, 1.0, 1.1, and 1.2 mm), insert types (mist sprayer -MSp and small sprayer - SSp), nozzle heights (0.5, 1.0, and 1.5 m) and, vertical positions (upright and inverted). The nozzle height setup resulted in a larger range in the radius of throw for the SSp positioned upright (23.4%) than inverted (1.3%), for the MSp, these variations were from 0.7 to 2.9%. Six geometric shapes of the dimensionless water distribution curve were sufficient to characterize the micro-sprinkler working with MSp and SSp. Running out the water distribution simulations for different spacings in rectangular and triangular layouts, it was found that: the MSp, regardless of the

Recebido em 24/08/2021 e aprovado para publicação em 20/10/2021
DOI: http://dx.doi.org/10.15809/irriga.2021v26n4p867-883

height and position of the micro-sprinkler, with spacings closer than 50% of the wetted diameter (WD), results in high values of uniformity coefficient (UC), and; for the SSp, the micro-sprinkler inverted position should be preferred, since results in high UC values for spacings up to 60% of WD.

Keywords: nozzle height, working pressure, nozzle diameter.

3 INTRODUCTION

Microsprinkler irrigation is characterized by the application of sprayed water through emitters (microsprinklers), which operate at a service pressure of approximately 200 kPa and flow rates of 20--150 L h^{-1} (BERNARDO *et al*., 2019). The adoption of this type of irrigation system is linked mainly to lower water and energy consumption and high water application efficiency (PRADO *et al*., 2021; FERNANDES *et al*., 2022).

In addition to replenishing crop water demand, microsprinkler irrigation can be used to reduce the air temperature near plants, consequently contributing to crop physiological development (LIU *et al*., 2021). The aforementioned authors reported that spray application (2, 4, and 6 mm day^{-1}) via microsprinklers reduced the average air temperature by 1--3°C and increased the relative humidity by 11--17%. This resulted in increased productivity and increased amounts of sugar and soluble solids in the fruits of the evaluated crop (*Jujube–Ziziphus). jujube*).

According to Bortoluzzi and Prado (2017), microsprinkler irrigation can be used in open fields and protected crop cultivation. Under field conditions, microsprinklers typically operate alone, without lateral overlap, and with rotating inserts, which provide a greater spray range. However, in greenhouses, microsprinklers are usually used in combination, inverted, suspended, or with fixed inserts (flat or grooved plates), which results in smaller wetted diameters.

Different operating combinations (operating pressure, nozzle diameter, insert type, and installation height) result in different geometric shapes for the microsprinkler's radial water distribution profile. For microsprinklers operating individually, operating conditions should be sought that result in radial profiles with a uniform geometric shape (F profile of CHRISTIANSEN, 1942) and that provide high uniformity coefficient values (BORTOLUZZI; PRADO, 2017).

In contrast, for sprinklers or microsprinklers that operate together, operating conditions must be selected that promote gradual decreases in the water application rate along the emitter's reach (profiles A, B and C of CHRISTIANSEN, 1942) so that the uniformity of water application is maximized with the occurrence of lateral overlap (PRADO, 2016).

Water application uniformity represents the dispersion of the water depths in relation to the average water depth. The smaller the dispersion is, the smaller the areas irrigated in excess or deficit (FERREIRA *et al*., 2016). These uniformity values (coefficients) can be obtained after the implementation of the irrigation system, from field evaluations (IQBAL *et al*., 2021), or prior to the implementation of the irrigation system through digital simulations with the radial profiles of the emitters (BORTOLUZZI; PRADO, 2017).

According to Pradeep *et al*. (2021), evaluations of the water distribution of microsprinkler systems are necessary to select the operating conditions that result in

adequate uniformity values. However, in the literature, most studies present results of evaluations of the water distribution of microsprinkler systems involving only the service pressure and spacing between microsprinklers (DWIVEDI; PANDYA, 2016; ANDRADE *et al*., 2017; PATEL *et al*., 2021).

Water distribution data for microsprinklers operating at different installation heights, installation methods, and nozzle diameters are scarce. Therefore, this study aimed to determine the water distribution characteristics of a microsprinkler operating under different operating conditions (operating pressure, nozzle diameter, insert type, installation height, and microsprinkler position) and to evaluate the results of simulations of water application uniformity for different microsprinkler operating situations.

4 MATERIALS AND METHODS

The work was carried out at the State University of Maringá, Arenito Campus, in Cidade Gaúcha, PR. This study evaluated the water distribution characteristics and range of microsprinklers. Naan Hadar®, model 7110, operates under different operating conditions.

The water distribution characteristics and the microsprinkler throw radius were determined for 144 operating conditions: i) three operating pressures (10, 15, and 20 mca), expressed in relation to the specific weight of water (γ = 1,000 kgf m $^{-3}$); ii) four nozzle diameters (0.9 mm - gray; 1.0 mm - purple; 1.1 mm - red; and; 1.2 mm - orange); iii) two types of diffuser inserts (nebulizers and short throws); iv) three microsprinkler nozzle installation heights in relation to the top of the collectors (0.5; 1.0, 1.5 m); and two microsprinkler operating positions (up and down).

Prior to the water distribution tests, the flow rate *versus* operating pressure ratios of the microsprinkler were determined. In these tests, to minimize the effect of pressure variations along the emitter line, a 1 1/2" rigid PVC line with an internal diameter of 40.1 mm and a length of three meters was used. Five connectors for connecting the microsprinkler nozzles, spaced 0.265 m apart, were inserted into this line.

To determine the flow rate, via the ponderal or weight method, microsprinkler nozzles (0.9, 1.0, 1.1, and 1.2 mm) were subjected to increasing pressures (10, 15, and 20 mca). The pressures were regulated via a drawer valve and monitored with a digital pressure gauge on a scale of 0--5 kgf cm^{-2}, with a pressure tap coupled in the center of the line. The emission flow rate of each microsprinkler nozzle, for a given operating pressure, was the average flow rate of the five emitters evaluated.

In the microsprinkler water distribution tests, the water collector mesh method was adopted, in accordance with the ISO 8026 technical standard (ISO, 2009), with the collectors distributed around the microsprinkler with a spacing of 0.3 × 0.3 m. These plastic collectors, with a collection diameter of eight centimeters, were installed in a flat, covered area, and the tests were carried out indoors in the absence of wind.

To measure the microsprinkler operating pressure, a pressure gauge installed at the height of the microsprinkler nozzle was used with a drawer valve. Pressures were checked every 15 minutes during the tests. Each test lasted approximately one hour, and the water volumes contained in the collectors were converted into water application intensities.

As suggested by Bortoluzzi and Prado (2017), at the end of each test, the flow rate determined as a function of the operating pressure was compared with the collected flow rate. The collected flow rate

corresponds to the sum of the product of the application intensities observed in each collector multiplied by the area of influence of each collector (0.09 ^{m2}).

In cases where there were differences between the collected and applied flow values, to avoid volumetric errors in the simulations, the observed water application intensity values were corrected by the ratio between the collected and applied flows.

The application intensity data observed in each collector grid were used to establish the microsprinkler range, which represents the farthest point where the intensity of 0.13 mm h $^{-1}$ ^{occurs}, in accordance with the ISO 8026 standard (ISO 2009).

The discharge flow and radius values of the microsprinkler for the different operational conditions were adjusted via the least squares method, according to Equations (1) and (2).

$$Q = a_1 * b^{a2} * p^{a3} \quad (1)$$

$$R = a_4 * h^{a5} * b^{a6} * p^{a7} \quad (2)$$

where Q is the discharge flow rate (L h $^{-1}$); R is the radius of reach (m); b is the nozzle diameter (mm); p is the service pressure (mca); h is the installation height in relation to the water application point (m); and a $_1$, a $_2$, a $_3$, a $_4$, a $_5$, a $_6$ and a $_7$ are the adjustment constants of the equations.

In relation to the radius of reach obtained with the microsprinkler installation height of 1.5 m, for a given service pressure (p) and nozzle diameter (b), the decrease in the radius of reach was calculated (PRADO *et al*., 2013) with the reduction in the microsprinkler installation height according to Equation 3.

$$DR = \frac{\left(R_h - R_{1,5}\right)}{R_{1,5}} * 100 = \left[\left(\frac{h}{1,5}\right)^{a5} - 1\right] * 100 \quad (3)$$

where DR is the decrease in the microsprinkler radius of reach (%); R $_h$ is the microsprinkler radius of reach for the installation height h (m); and R $_{1.5}$ is the microsprinkler radius of reach for the height of 1.5 m.

The corrected application intensity data (mm h $^{-1}$) in the collector grid were used to construct the radial profiles of the microsprinkler operating under different operating conditions. For this procedure, the average of the application intensity values observed at the same radial distance from the microsprinkler was determined.

The water distribution profiles were dimensionless according to the methodology presented by Solomon and Besdek (1980), in which the distances to the microsprinkler are expressed in terms of the fraction of the radius of reach (Equation (4)) and the application intensity values in terms of the fraction of the average water application intensity (Equation (5)).

$$ra_j = \frac{dr_j}{R} \quad (4)$$

$$ia_j = \frac{ip_j * \pi * R^2}{Q} \quad (5)$$

where ra j is the fraction of the microsprinkler radius (dimensionless); ia $_j$ is the fraction of the average water application intensity (dimensionless); dr $_j$ is the radial distance of a sampling point j in relation to the microsprinkler (m); and ip $_j$ is the water intensity at a sampling point j (mm h $^{-1}$).

With the information obtained from each radial water distribution profile, twenty values of dimensionless precipitation intensity corresponding to twenty fractions of the radius of reach (ra_t) were generated via interpolation with a cubic *spline* (BURDEN; FAIRES, 2003), Equation (6).

$$ra_t = 0{,}025 + (t-1) * 0{,}05 \quad (6)$$

where t is the identification index that varies from 1 to 20.

To identify typical geometric shapes assumed by the dimensionless radial profiles, the seventy-two dimensionless radial profiles for each type of microsprinkler insert were subjected to cluster analysis via the *K-means algorithm* (PRADO; COLOMBO, 2005).

For the simulations of lateral overlap as a function of the spacing between microsprinklers, in the rows and between rows, from 30--100% of the wetted diameter of the microsprinkler, and the calculation of the application uniformity via the Christiansen uniformity coefficient (CUC), a computational routine was developed, written in *Visual Basic for applications in the Excel* spreadsheet, as described by Prado (2016).

The water application uniformity values as a function of the spacing in the row and between rows are represented in contour graphs, in which the operational conditions that promote the best uniformity values (CUC > 80%) (BERNARDO *et al*., 2019) of the micro sprinkler are indicated, operating with the nebulizer insert and with the short-range insert.

In all the generated contour plots, the curve that delimits the spacing combinations between microsprinklers, from which the overlap of the wetted areas is incomplete, was plotted. The spacing combinations between microsprinklers from which the complete coverage of the irrigated area begins to be compromised were determined for rectangular and triangular arrangements (PRADO, 2016) via Equations (7) and (8).

$$\frac{Sl}{DM} = \sqrt{1 - \left(\frac{Sp}{DM}\right)^2} \quad (7)$$

$$\frac{Sl}{DM} = \sqrt{1 - 4 * \left(\frac{Sp}{DM} - 0{,}5\right)^2} \quad (8)$$

where Sl is the spacing between microsprinklers in the line (m); Sp is the spacing between microsprinklers in the line (m); and DM is the wetted diameter of the microsprinkler (m).

5 RESULTS AND DISCUSSION

Figure 1 shows the discharge flow rate *versus* operating pressure values for the four nozzles of the microsprinkler evaluated. Notably, with increasing operating pressure, for all the nozzles evaluated, the emitter discharge flow rate increases.

Figure 1. The microsprinkler discharge flow rate as a function of the nozzle diameter (b in mm) and operating pressure (p in mca).

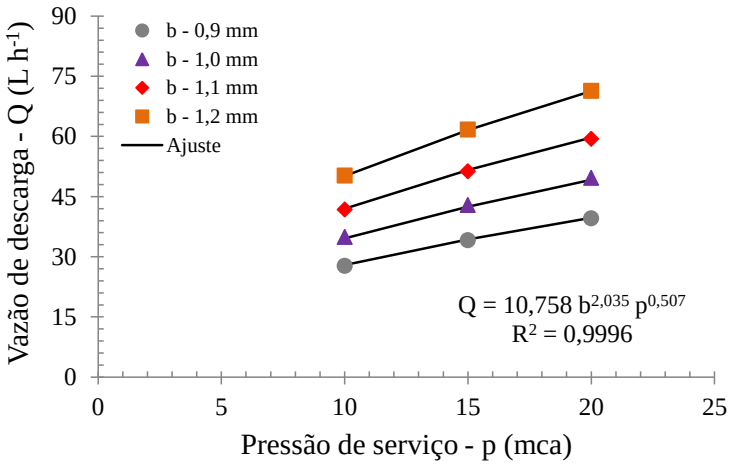

For the flow values observed in the tests, a potential equation was adjusted as a function of the nozzle diameter and the operating pressure (Figure 1). When this equation was adjusted, a coefficient of determination close to unity was observed (R^2 = 0.9996), revealing that the observed data fit the potential model well (PRADO *et al*., 2021). The pressure exponent of 0.507 in this equation reveals that the tested microsprinkler can be classified as a turbulent regime emitter (FRIZZONE *et al*., 2012).

In the water distribution tests of the microsprinkler operating with the nebulizer insert, variations in the reach radii of 1.06 to 1.29 m and 1.06 to 1.36 m were observed for the microsprinkler installed vertically upward and downward, respectively. In contrast, for the short-reach insert, these variations were 1.10 to 1.96 m with the microsprinkler installed upward and 1.66 to 2.21 m downward. For these observed data, the equations were adjusted to estimate the reach radius as a function of the nozzle height in relation to the collectors, nozzle diameter and microsprinkler operating pressure (Table 1).

Table 1. Equations of the range radius (R in m) of the microsprinkler in the upper and lower positions with the nebulizer and small range inserted as a function of the nozzle diameter (b in mm), the operating pressure (p in mca) and the installation height (h in m).

Insert	Position	Equation	R^2
Nebulizer	Up	$R = 0{,}7163 * h^{0{,}0270} * b^{0{,}3731} * p^{0{,}1598}$	0.5588
	Low	$R = 0{,}8521 * h^{0{,}0065} * b^{0{,}3226} * p^{0{,}1363}$	0.5771
Small range	Up	$R = 1{,}0770 * h^{0{,}2432} * b^{0{,}7441} * p^{0{,}1187}$	0.9372
	Low	$R = 1{,}5076 * h^{0{,}0120} * b^{0{,}5222} * p^{0{,}0835}$	0.7714

The smallest variations in the radius of reach of the microsprinkler operating with the nebulizing insert provided coefficients of determination of the equations of 55.88% (upward position) and 57.71% (downward position) (Table 1). On the other hand, the largest variations in the observed values of the radius of reach for

the small-range insert resulted in coefficients of determination of the equations of 93.72% (upward position) and 77.14% (downward position). Bortoluzzi and Prado (2017), when adjusting the radius equations for the same microsprinkler operating with rotary inserts, observed coefficients of determination values that varied between 68.9 and 88.7%.

According to Ouazaa *et al*. (2014), the larger the spray of a sprinkler's water jet is, the smaller the droplet size produced, resulting in a smaller wetted area. Thus, owing to the larger spray provided by the microsprinkler operating with the nebulizer insert (smooth plate), the decrease in range when the installation height was reduced, regardless of the emitter position, was not as pronounced (Figure 2). By reducing the microsprinkler installation height from 1.5 m to 0.5 m, reductions of 2.9 and 0.7% in the range were observed for microsprinklers positioned vertically upward and downward, respectively.

Figure 2. Decrease in the range for the nebulizer (INeb) and short-range (IPalc) inserts as a function of the reduction in the height and installation position of the microsprinkler.

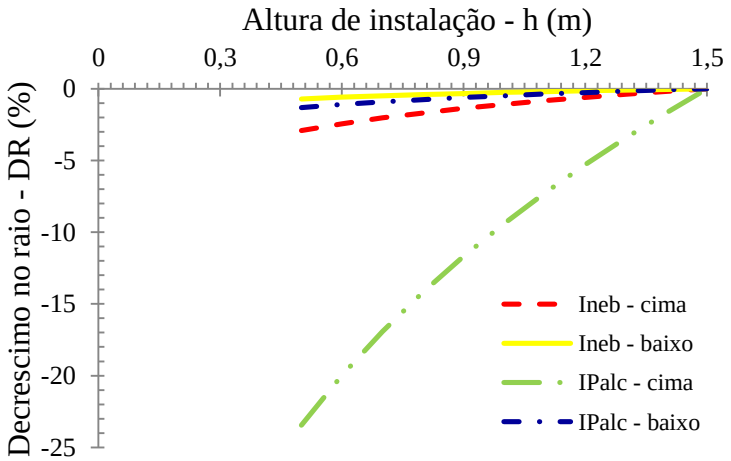

For the microsprinkler operating with the short-range insert (concave grooved plate) installed vertically downward with the concavity facing upward, the reduction in range was also not as pronounced (1.3%) when the installation height was reduced (Figure 2). However, when the microsprinkler was installed vertically upward, with the concavity of the insert facing downward, this decrease in range was pronounced (23.4%). In central pivot irrigation systems, fixed grooved plates are usually used with the concavity facing upward (SOBENKO *et al*., 2019; ZHANG *et al*., 2019).

The results of the cluster analysis (*K-means*) of the dimensionless radial profiles of the water distribution are presented in Figure 3. This cluster analysis was performed separately with the dimensionless radial profiles obtained under the operational conditions of installation height, microsprinkler position, nozzle diameter and pressure for the nebulizer insert (72 profiles) and for the short-range insert (72 profiles).

Figure 3. Average error in relation to the number (K) of representative profiles employed.

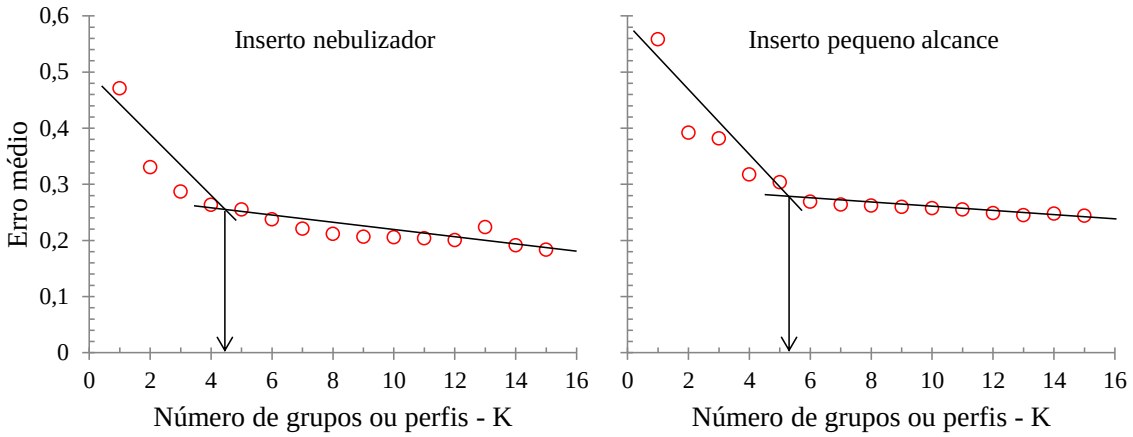

In accordance with Solomon and Bezdek (1980), the number of profiles is chosen near the inflection point between the mean error and the number K of profiles (Figure 3). Thus, when establishing six radial profiles (K = 6) for the operating conditions of the nebulizer and short-range inserts, the mean error in the dimensionless application intensity varied from 0.24 to 0.27, and from that point (K = 6), with the increase in the number of "K" profiles, the mean error decreased until a value equal to zero (K = 72) was assumed. Prado (2016), when 16 dimensionless radial profiles of a medium-sized sprinkler were grouped into three typical profiles, obtained a mean error equal to 0.19.

Figures 4 and 5 show the dimensionless radial profiles representing the operating conditions of the microsprinkler operating with the nebulizer and short-range inserts, respectively. The vertical bars in these two figures represent an error of plus or minus one standard deviation in the dimensionless intensity value obtained at each point.

Figure 4. Representative dimensionless profiles of the microsprinkler operating with the nebulizer insert.

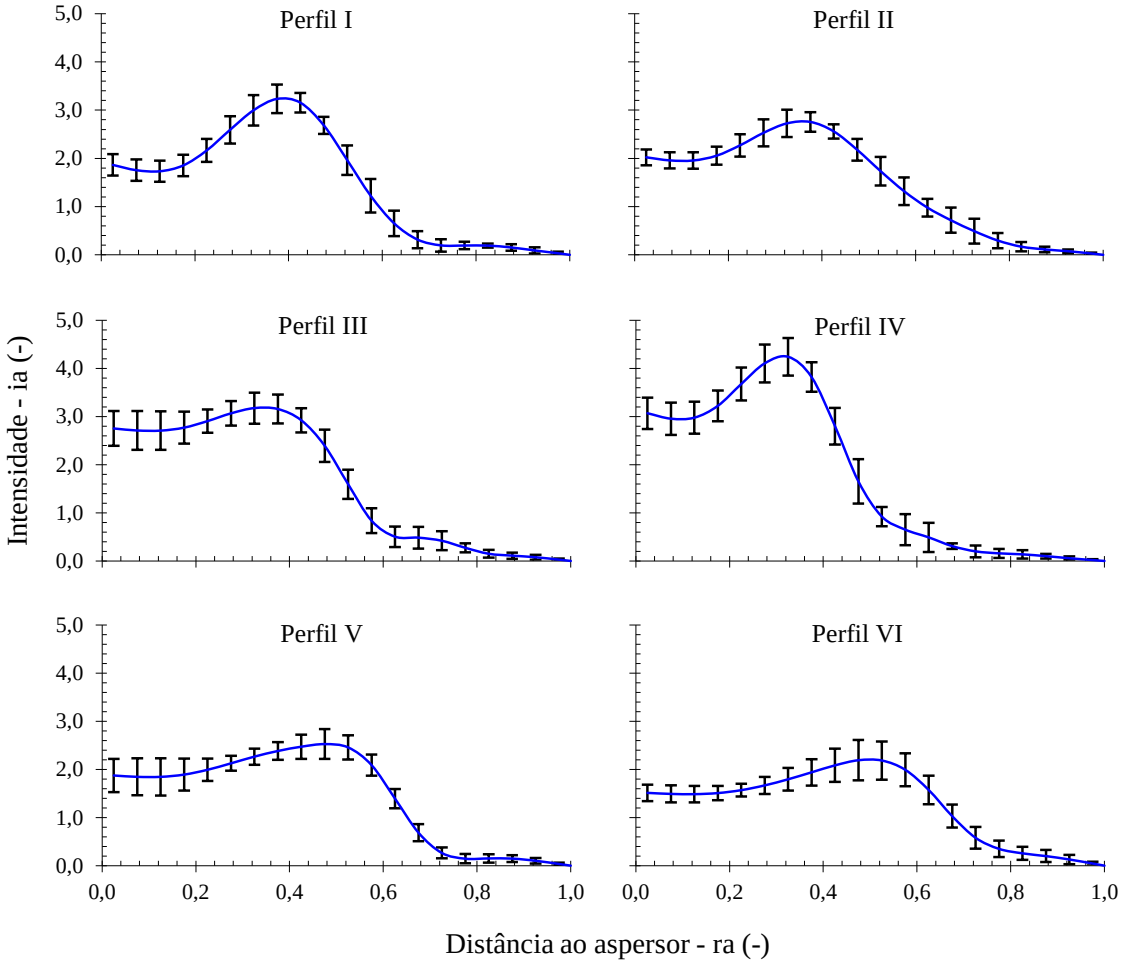

Figure 5. Representative dimensionless profiles of the microsprinkler operating with the short-range insert.

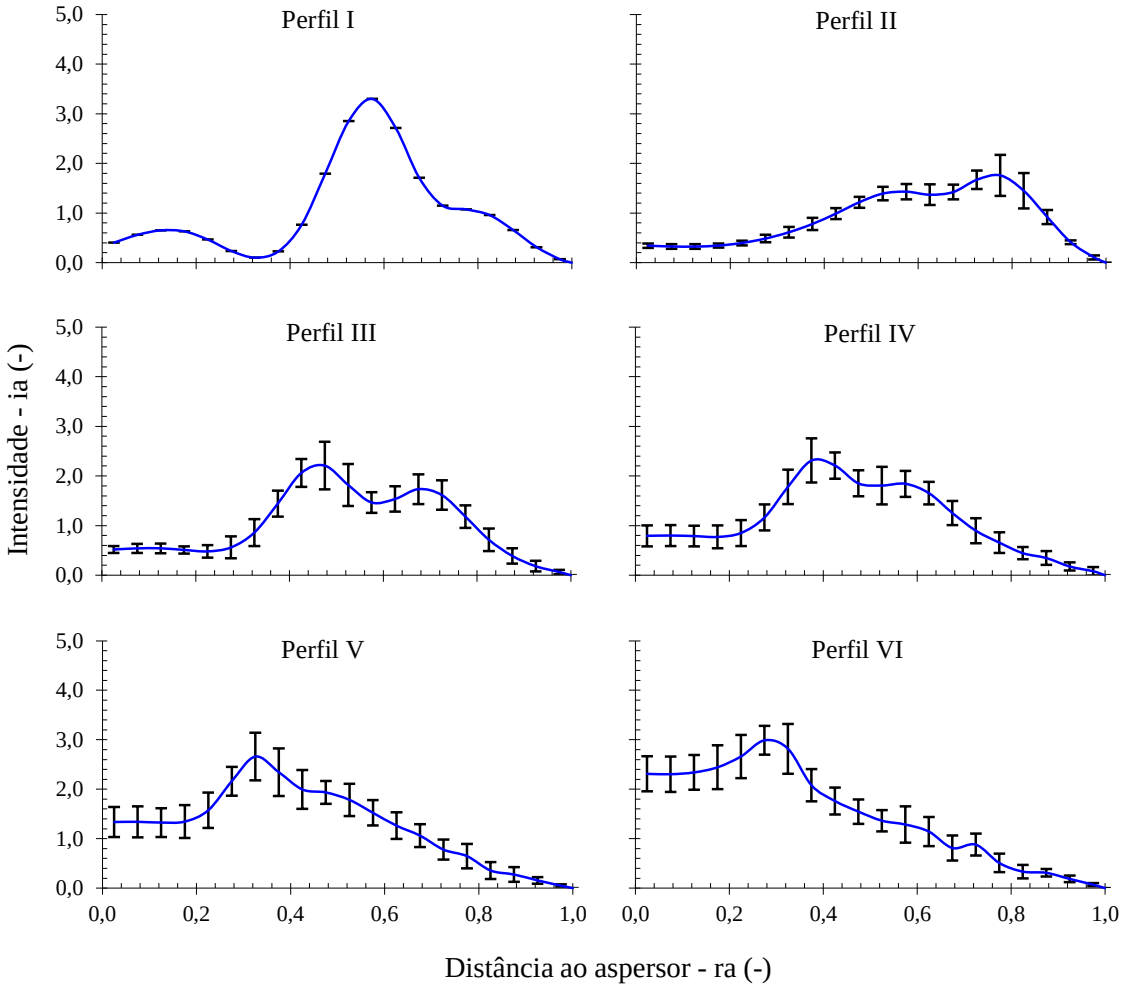

The geometric shapes assumed by the dimensionless radial profiles obtained under different operating conditions of the microsprinkler operating with a nebulizer insert (Figure 4), in the range between 0.3 and 0.6 of the radius fraction, show an increase in the water application intensity values. For geometric shapes I and IV, this increase in application intensity was more pronounced than that for the other geometric shapes (II, III, V, and VI). After this increase, the application intensity values decrease to zero, which is a typical characteristic of Christiansen's theoretical geometric shapes A, B, and C (CHRISTIANSEN, 1942).

With the exception of geometric shapes V and VI, the radial profiles obtained under different microsprinkler operating conditions, working with the short-range insert, presented low water application intensity values near the microsprinkler (ia < 1). As the distance from the microsprinkler increases, these values increase sharply, reach a peak, and decrease again (Figure 5). According to Bortoluzzi and Prado (2017), operating conditions that provide this type of radial profile, known as a donut profile, should be avoided, as they result in inadequate water application uniformity values. However, geometric shapes V and VI resemble profiles A, B, and C described by Christiansen (CHRISTIANSEN, 1942).

Tables 2 and 3 define the operating conditions (emitter position × installation

height × nozzle diameter × operating pressure) of the microsprinkler operating with the nebulizer and short-range inserts belonging to each group (I, II, III, IV, V, and VI). By identifying the dimensionless profile representative of the operating condition of interest, with the range radius and water application intensity data, it is possible to proceed with the dimensioning of the radial water distribution profile.

Table 2. Representative profiles of the microsprinkler operating with the nebulizer inserted in the upper and lower positions as a function of the nozzle diameter (b), operating pressure (p) and installation heights of 0.5 (h1), 1.0 (h2) and 1.5 m (h3).

b	p	Upward position			Down position		
(mm)	(mca)	h 1	h 2	h 3	h 1	h 2	h 3
0.9	10	I	III	I	I	II	III
	15	I	III	III	IV	II	IV
	20	II	III	II	IV	III	IV
1.0	10	I	II	II	III	III	V
	15	V	II	II	IV	III	III
	20	VI	I	II	III	III	III
1.1	10	V	V	V	I	I	IV
	15	VI	VI	II	III	III	III
	20	VI	II	II	III	II	III
1,2	10	VI	VI	V	I	III	IV
	15	V	VI	II	II	II	II
	20	VI	V	V	V	VI	V

Table 3. Representative profiles of the microsprinkler operating with the short-range insert in the upper and lower positions as a function of the nozzle diameter (b), operating pressure (p) and installation heights of 0.5 (h1), 1.0 (h2) and 1.5 m (h3).

b	p	Upward position			Down position		
(mm)	(mca)	h 1	h 2	h 3	h 1	h 2	h 3
0.9	10	I	III	III	IV	V	IV
	15	II	IV	IV	IV	V	V
	20	II	IV	IV	V	V	V
1.0	10	II	III	III	V	V	V
	15	III	IV	IV	V	VI	VI
	20	III	IV	IV	VI	VI	VI
1.1	10	III	III	IV	V	V	V
	15	III	IV	IV	VI	VI	V
	20	III	IV	IV	VI	VI	V
1,2	10	III	IV	V	V	V	V
	15	III	V	V	VI	VI	VI
	20	III	IV	V	VI	VI	VI

According to Solomon and Bezdek (1980) and Prado (2016), certain emitter operating conditions tend to present a specific geometric shape of the radial water distribution profile. For the nebulizer insert, this is not as evident, but geometric shape I appears more frequently for low operating pressure conditions (p = 10 mca) and geometric shapes V and VI for higher pressures (Table 2).

When considering the geometric shapes of the radial profile for the short-range insert (Table 3), it is clear that geometric shapes I, II, III and IV are more frequent for the conditions of the microsprinkler installed vertically upward and, for the emitter placed vertically downward, only geometric shapes IV, V and VI occur.

The representative radial profiles, presented in Figures 4 and 5, were used to simulate the water distribution of microsprinklers operating in tandem for different emitter spacings, expressed in terms of wetted diameter (WD). Using the lateral overlap values between emitters, for spacings in rectangular (Figures 6 and 8) and triangular (Figures 7 and 9) arrangements, the Christiansen uniformity coefficients (CUC) were determined. In Figures 6, 7, 8, and 9, the spacing combinations below the yellow dotted line ensure minimal overlap between microsprinklers.

Figure 6. Christiansen uniformity coefficients (CUC) of the microsprinkler operating with the nebulizer insert for emitter spacing in a rectangular arrangement.

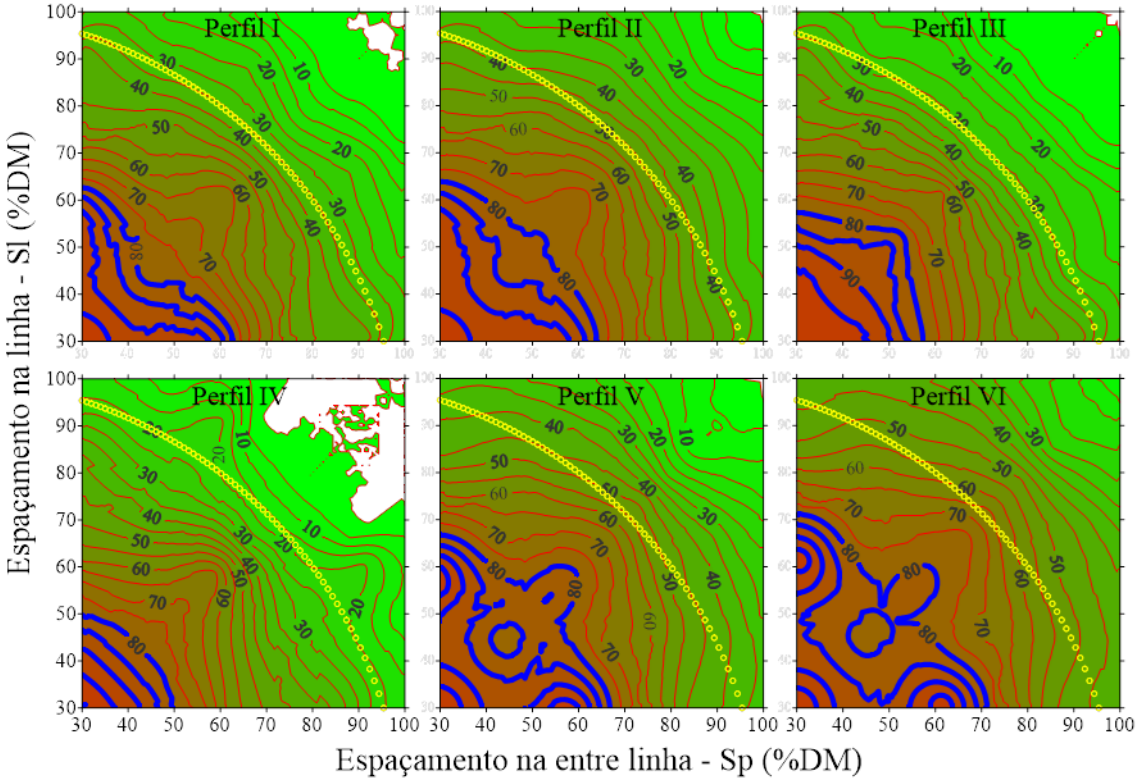

Figure 7. Christiansen uniformity coefficients (CUC) of the microsprinkler operating with the nebulizer insert for emitter spacing in a triangular arrangement.

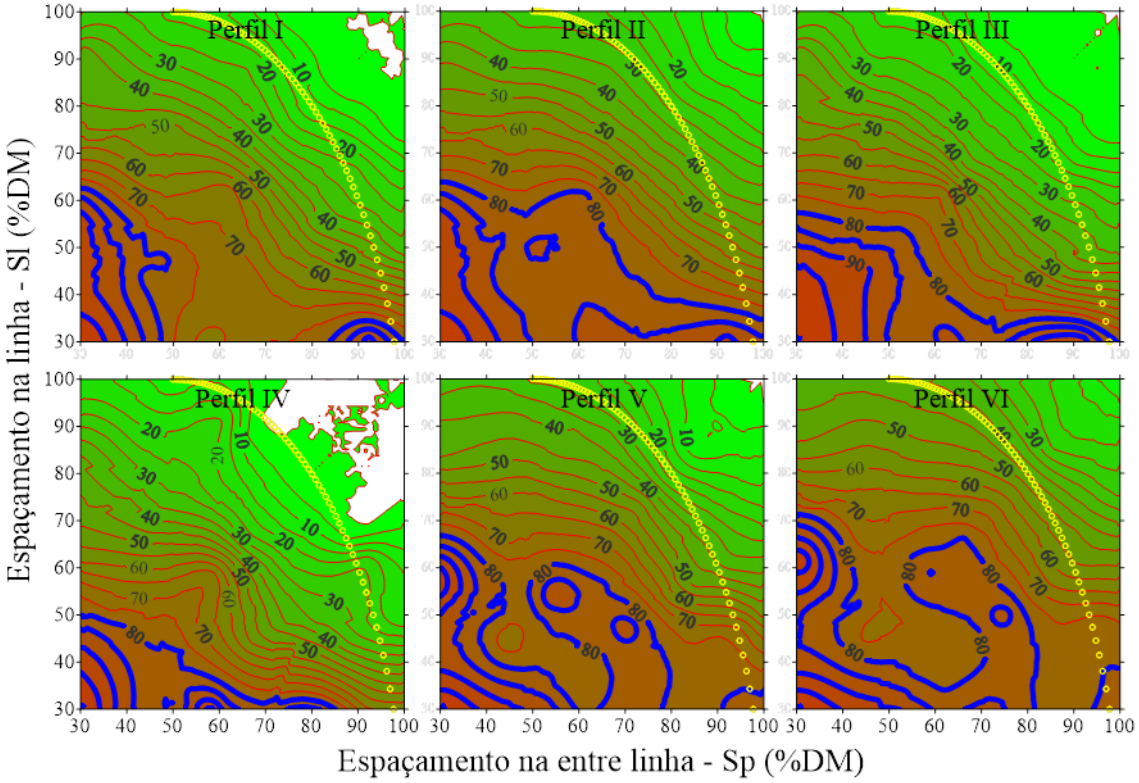

Figure 8. Christiansen uniformity coefficients (CUC) of the microsprinkler operating with the short-range insert for emitter spacings in a rectangular arrangement.

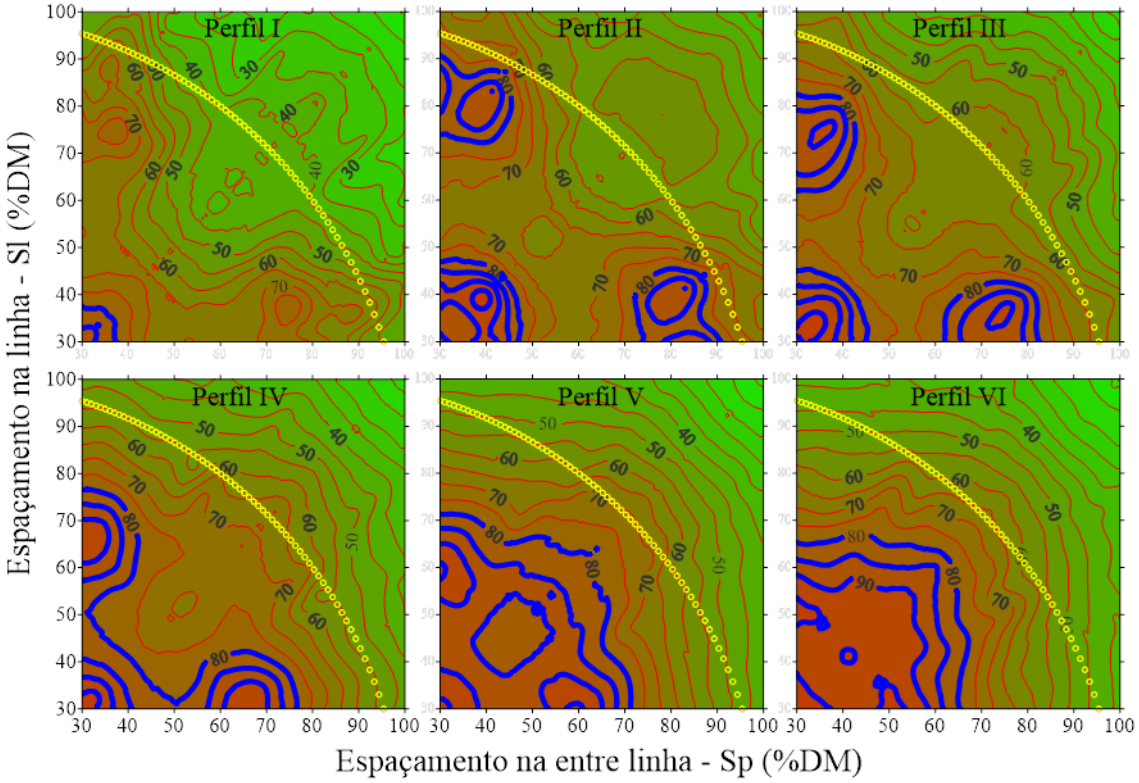

Figure 9. Christiansen uniformity coefficients (CUC) of the microsprinkler operating with the short-range insert for emitter spacings in a triangular arrangement.

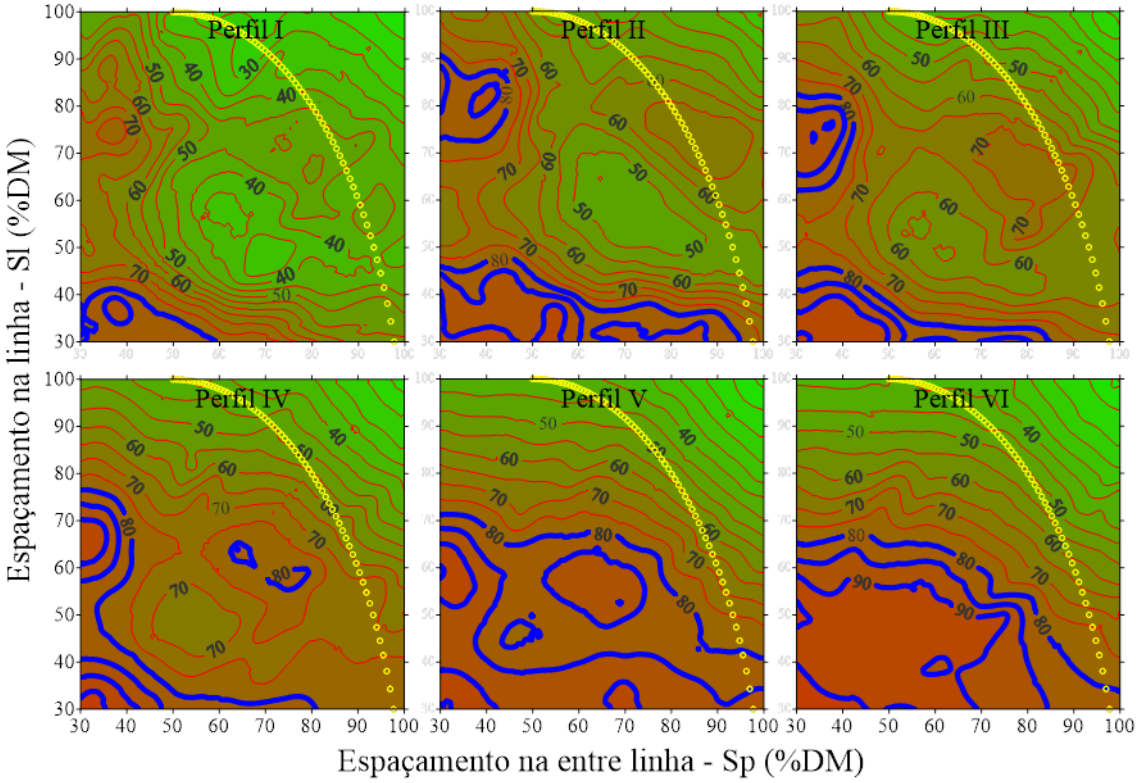

As presented in the literature (BERNARDO *et al*., 2019; FRIZZONE *et al*., 2012; PRADO, 2016), Christiansen uniformity coefficient values equal to or greater than 80% provide adequate water distribution from emitters. However, operating conditions that result in greater spacing between microsprinklers promote lower irrigation project costs and should be preferred.

In general, for the microsprinkler operating with the nebulizer insert, regardless of the arrangement between microsprinklers, spacings, both in the line (Sl) and between the lines (Sp), less than 45% of the microsprinkler's DM, result in adequate CUC values (Figures 6 and 7). Exceptions to this are operating conditions that result in radial profiles with geometric shapes V and VI for the rectangular and triangular arrangements and II for the triangular arrangement. Under these conditions, spacings equal to or less than 50% of the DM in the line (Sl) and equal to or less than 60% of the DM between the lines (Sp) generate CUC values greater than 80% (Figures 6 and 7).

For the geometric shapes of radial profiles I, II, III, and IV obtained with the short-range insert (Figure 5), very close spacings (less than 40% of the DM) must be used to generate CUC values greater than 80% (Figures 8 and 9). Owing to the low CUC values obtained with the representative profile I (Table 3), these microsprinkler operating conditions should be avoided.

The operating conditions that lead to representative profiles V and VI, in rectangular arrangements, allow high values of uniformity coefficients with spacings smaller than 60% of the wetted diameter to be achieved (Figure 8). On the other hand, for triangular arrangements (Figure 9), spacings in the line (Sl) equal to or less than 60% of the DM and spacings in the line (Sp) equal to or less than 70% of the DM provide adequate CUC values (CUC >

80%).

Reducing the spacing between microsprinklers improves water application uniformity (ANDRADE *et al*., 2017; PATEL *et al*., 2021). This closer proximity between emitters leads to greater water application intensity and increased irrigation system installation costs. Therefore, operational combinations that allow for greater spacing between emitters should be prioritized.

6 CONCLUSIONS

The results indicate that i) operating conditions with the short-range insert provided larger range radii; ii) variations in the range radius with the short-range insert, installed vertically upward, were more pronounced; iii) six geometric shapes are sufficient to represent the radial profiles of the microsprinkler operating with the nebulizing and short-range insert; iv) spacing between emitters close to 50% of the wetted diameter resulted in adequate CUC values in most of the situations evaluated; and v) the use of the short-range insert with the microsprinkler installed vertically upward should be avoided.

7 REFERENCES

ANDRADE, MG; VILAS BOAS, MA; SIQUEIRA, JAC; SATO, M.; DIETER, J.; HERMES, E.; MERCANTE, E. Uniformity microsprinkler irrigation system using statistical quality control . **Rural Magazine** , Santa Maria, v. 47, no. 4, p. 1-7, 2017.

BERNARDO, S.; MANTOVANI, EC; SILVA, DD; SOARES, AA; **Irrigation Manual** . 9th ed . Viçosa: UFV Publishing House, 2019. 545 p.

BORTOLUZZI, DD; PRADO, G. Modeling of water distribution from microsprinklers. **Brazilian Journal of Irrigated Agriculture** , Fortaleza, v. 11, n. 7, p. 2063-2075, 2017.

BURDEN, R.L.; FAIRES, J.D. **Numerical analysis** . New York: Pioneira Thomson Learning, 2003. 740 p.

CHRISTIANSEN, JE **Irrigation by sprinkling** . Berkeley: California Agricultural Station, 1942. 124 p. Bulletin, 670

DWIVEDI, DK; PANDYA, PA Evaluation of hydraulic performance of microsprinkler irrigation . **International Journal of Agricultural Science and Research** , Rochester, vol. 6, no. 3, p. 397-406, 2016.

FERNANDES, GST; MORALES, KRM; PESSOA, VG; OLIVEIRA, VB; LIMA, EA; SILVA, TGP Simulation of the energy gradient of the lateral line with type MF2 microsprinkler. **Brazilian Journal of Irrigated Agriculture** , Fortaleza, v. 16, n. 1, p. 21-30, 2022.

FERREIRA, LLN; LEMOS FILHO, LC; TORRES, MM; OLIVEIRA JUNIOR, RF; VALE, CNC; FRANCO, MSBP Spatial variability of available water and microsprinkler irrigation in cambisol . **Ceres Magazine** , Viçosa, v. 63, n. 6, p. 782-788, 2016.

FRIZZONE, JA; FREITAS, PSL; REZENDE, R.; FARIA, MA **Microirrigation: drip and microsprinkler** . Maringá : Eduem , 2012. 356 p.

INTERNATIONAL ORGANIZATION FOR STANDARDIZATION. ISO 8026. **Agricultural irrigation equipment – Sprayers: General requirements and test methods** . Geneva, 2009. 18p.

IQBAL, U.; AHMAD, I.; ZAMAN, M.; KHAN, NM; SARWAR, MK Performance evaluation of micro sprinkler irrigation system in tunnel farms and open area conditions . **Fresenius Environmental Bulletin** , Freising, vol. 30, no. 3, p. 2888-2898, 2021.

LIU, Z.; JIAO, X.; Zhu, C.; KATUL, GG; MA, J.; GUO, W. Microclimatic and crop response to microsprinkler irrigation. **Agricultural Water Management** , Amsterdam, v. 243, p. 1-11, 2021.

OUAZAA, S.; BURGUETTE, J.; PANIAGUA, MP; SALVADOR, R.; ZAPATA, N. Simulating water distribution patterns for fixed spray plate sprinkler using the ballistic theory . **Spanish Journal of Agricultural Research** , Madrid, v. 12, no. 3, p. 850-863, 2014.

PATEL, RJ; VEKARIYA, PB; VADAR, HR; RANK, HD; PANDYA, PA; MODHAVADIA, JM Hydraulic performance evaluation of double nozzle full circle microsprinkler irrigation system under semiarid conditions . **International Research Journal of Modernization in Engineering Technology and Science** , Indore, vol. 3, no. 1, p. 39-50, 2021.

PRADEEP, SA; GOVIND, DS; DHARMARAJ, JK; SURESH, KA Performance evaluation of micro sprinkler system . **International Journal of Current Microbiology and Applied Sciences** , Kancheepuram, vol. 10, no. 1, p. 1630-1635, 2021.

PRADO, G. Water distribution from medium-size sprinkler in solid set sprinkler systems. **Brazilian Journal of Agricultural and Environmental Engineering** , Campina Grande, v. 20, n. 3, p. 195-201, 2016.

PRADO, G.; BRUSCAGIN, RR; TINOS, AC; BORTOLETTO, EC; MAHL, D. Iterative calculation of local head loss coefficient of emitter in lateral lines. **Brazilian Journal of Agricultural and Environmental Engineering** , Campina Grande, v. 25, n. 5, p. 291-296, 2021.

PRADO, G.; FARIA, LC; OLIVEIRA, HFE; COLOMBO, A. Effect of jet angle on the technical characteristics of a hydraulic cannon. **Brazilian Journal of Agricultural and Environmental Engineering** , Campina Grande, v. 17, n. 7, p. 689-697, 2013.

PRADO, G.; COLOMBO, A. Technical characterization of the PLONA-RL300 sprinkler. **Irriga** , Botucatu, v. 10, n. 1, p. 53-63, 2005.

SOBENKO, LR; CAMARGO, AP; BOTREL, TA; FRIZZONE, JA; OLIVEIRA, MF; LAVANHOLI, R.; SANTOS, JDM DUARTE, SN Performance of an iris mechanism equipped with fixed and rotating deflector plates for variable rate sprinkler irrigation . **Journal of Irrigation and Drainage Engineering** , New York, vol. 145, no. 12, p. 1-10, 2019.

SOLOMON, K.; BEZDEK, JC Characterizing sprinkler distribution patterns with a clustering algorithm. **Transactions of the American Society of Agricultural Engineers** , St. Joseph, vol. 23, p. 899- 906, 1980.

ZHANG, Y.; GUO, J.; SUN, B.; FANG, H.; Zhu, D.; WANG, H. Modeling and dynamic-simulating the water distribution of a fixed spray-plate sprinkler on a lateral-move sprinkler irrigation system . **Water** , Basel, vol. 11, no. 1, p. 1-16, 2019.